Nagra
Nationale
Genossenschaft
für die Lagerung
radioaktiver Abfälle

Cédra
Société coopérative
nationale
pour l'entreposage
de déchets radioactifs

Cisra
Società cooperativa
nazionale
per l'immagazzinamento
di scorie radioattive

TECHNICAL REPORT 85-36

GAS MIGRATION THROUGH MX-80 BENTONITE

Final Report

R. Pusch
L. Ranhagen
K. Nilsson

January 1985

Swedish Geological, Lund, Sweden

Parkstrasse 23 5401 Baden/Schweiz Telephon 056/20 55 11

Nagra
Nationale
Genossenschaft
für die Lagerung
radioaktiver Abfälle

Cédra
Société coopérative
nationale
pour l'entreposage
de déchets radioactifs

Cisra
Società cooperativa
nazionale
per l'immagazzinamento
di scorie radioattive

TECHNICAL REPORT 85-36

GAS MIGRATION THROUGH MX-80 BENTONITE

Final Report

R. Pusch
L. Ranhagen
K. Nilsson

January 1985

Swedish Geological, Lund, Sweden

Parkstrasse 23 5401 Baden/Schweiz Telephon 056/20 55 11

Der vorliegende Bericht wurde im Auftrag der Nagra erstellt. Die Autoren haben ihre eigenen Ansichten und Schlussfolgerungen dargestellt. Diese müssen nicht unbedingt mit denjenigen der Nagra übereinstimmen.

Le présent rapport a été préparé sur demande de la Cédra. Les opinions et conclusions présentées sont celles des auteurs et ne correspondent pas nécessairement à celles de la Cédra.

This report was prepared as an account of work sponsored by Nagra. The viewpoints presented and conclusions reached are those of the author(s) and do not necessarily represent those of Nagra.

SUMMARY

Highly compacted bentonite is known to let gas through at a very low rate but earlier investigations have indicated the possible existence of a critical gas pressure at which the gas forms highly conductive passages through the clay. The present study was primarily aimed at testing the hypothesis of the critical pressure concept by measuring the gas flow as a function of the applied, successively increased gas pressure, and by trying to identify microstructural evidence of how gas percolates clay.

Eight tests were run with MX-80 bentonite saturated with strongly brackish NAGRA water, the density of the water saturated bentonite ranging from 1.7 to somewhat more than 2.1 t/m^3. In all the tests it was observed that gas break-through, manifested by a largely increased conductivity, took place at a gas pressure of the same order of magnitude as the swelling pressure.

One of the samples was analysed with respect to the microstructure and it revealed the existence of discrete gas-filled voids, some of which released gas when the trimmed clay specimen was placed into the embedding substance used for the microstructural analysis. This confirms that gas percolates through a number of narrow passages that are formed when the gas pressure is sufficiently high. In soft and medium-dense bentonite the "capillary retention" is probably the major resistance to gas propagation, while in dense bentonite the penetrating gas has to make its way by displacing clay aggregates. In the latter case the critical gas pressure is therefore logically very high and close to the swelling pressure.

ZUSAMMENFASSUNG

Es ist allgemein bekannt, dass der Transport von Gasen durch hochkompaktierten Bentonit sehr langsam ist, doch weisen die Ergebnisse früherer Untersuchungen darauf hin, dass es einen kritischen Gasdruck gibt, bei welchem Pfade hoher Gasdurchlässigkeit im Ton entstehen. Ziel der vorliegenden Arbeit war es, die Hypothese des kritischen Gasdruckes durch Erfassung des Gasflusses als Funktion des stufenweise erhöhten Gasdruckes zu prüfen sowie allfällig vorhandene mikrostrukturelle Hinweise zum Mechanismus der Gasperkolation festzuhalten.

Es wurden acht Versuche an Bentonitproben vom Typ MX-80 durchgeführt, die mit dem verhältnismässig stark salzhaltigen Nagra-Referenzwasser zu Nassdichten zwischen 1.7 t/m^3 und etwas über 2.1 t/m^3 gesättigt wurden. Bei allen Versuchen wurde ein Schwelldruck für Gasdurchbruch beobachtet, welcher mit dem Quelldruck vergleichbar war, und mit welchem eine erhebliche Zunahme der Gasdurchlässigkeit verbunden war.

Die Mikrostruktur einer Probe wurde analysiert. Einzelne, gasgefüllte Blasen wurden beobachtet. Als die Probe in die zur mikrostrukturellen Analyse verwendete Substanz eingebettet wurde, setzten einige dieser Blasen Gas frei. Diese Tatsache bestätigt, dass das Gas durch mehrere enge Pfade perkoliert, welche bei ausreichendem Gasdruck entstehen. In Bentoniten niedriger und mittlerer Dichte leisten kapillare Kräfte wahrscheinlich den wichtigeren Beitrag zur Verhinderung des Gastransportes. In Bentoniten hoher Dichte hingegen muss das perkolierende Gas Tonplättchenaggregate verschieben. In diesem Fall liegt der erwartungsgemäss sehr hohe kritische Gasdruck nahe am Quelldruck.

RESUME

L'on sait que le transport des gaz à travers la bentonite fortement comprimée est très lent; des essais récents ont cependant donné à penser qu'il existe une pression de gaz critique à laquelle le gaz forme des passages de haute conductivité à travers la masse d'argile. La présente étude a été conçue dans le but de tester l'hypothèse de l'existence d'une pression de gaz critique en déterminant le flux gazeux en fonction de la pression de gaz appliquée, celle-ci étant augmentée par incréments discrets; de plus il était prévu d'étudier la microstructure afin de mettre éventuellement en évidence le mécanisme de percolation du gaz.

Huit essais ont été menés à bien sur des échantillons de bentonite de type MX-80 saturés avec l'eau de référence de la Cédra, de salinité relativement élevée. Les densités finales des échantillons saturés variaient entre 1.7 t/m^3 et un peu plus de 2.1 t/m^3. Au cours de tous les essais on a observé que la conductivité au gaz augmentait soudainement à partir d'une pression seuil du même ordre de grandeur que la pression de gonflement de l'échantillon.

L'un des échantillons a été soumis à une analyse de microstructure qui a révélé l'existence de poches bien définies et remplies de gaz; certaines d'entre elles ont laissé échapper du gaz lors du placement de l'échantillon dans la substance de support utilisée pour l'analyse de microstructure. Ceci confirme le fait qu'un phénomène de percolation du gaz a lieu à travers plusieurs passages étroits qui sont formés si la pression gazeuse est suffisante. Pour les bentonites de densité faible ou moyenne les effets de capillarité sont probablement responsables pour la résistance au transport du gaz, tandis que dans les bentonites de densité élevée le gaz doit déplacer les aggrégats d'argile. Il est ainsi logique que dans ce dernier cas la pression de gaz critique soit très élevée et proche de la pression de gonflement.

CONTENTS

1 INTRODUCTION

Earlier investigations have indicated that hydrogen as well as nitrogen gas under pressure penetrate water saturated, highly compacted bentonite at a very low rate (1). Thus, the gas conductivity was found to be of the same order of magnitude as the hydraulic conductivity, i.e. in the range of 10^{-13} to $2x10^{-14}$ m/s for the bulk density interval 1.86 to 2.05 t/m^3. These tests concerned MX-80 bentonite (2) saturated with distilled water, using a gas pressure of 1 MPa for the lowest density and about 10 MPa for the higher ones. After testing, the samples exposed to nitrogen gas were examined with respect to their water content and density and it then turned out that their degree of water saturation was not lower than 98 %, indicating that the gas had hardly replaced any water. The conclusion was that it had migrated in gaseous form through a small fraction of the cross section only. Later, it was correctly pointed out by Professor Ivars Neretnieks that an alternative explanation may be that the gas migration took place mainly through diffusion of dissolved gas.

Two observations were in strong support of the hypothesis that gas migrates mainly through a small number of more or less tortuous passages at higher pressures. One was that the hydrogen gas test, which was run on a 1.99 t/m^3 sample with a maximum gas pressure of 10 MPa, resulted in a sudden break-through after some time, thereby causing partial drying of the clay. The other was that such break-through occurs regularly in gas conductivity measurement of soft bentonite/ballast mixtures. In all these cases there seems to have been a critical gas pressure at which the gas abruptly made its way through a few passages in the samples. Once these had been formed, the gas seepage capacity became very high, and if this is a true phenomenon it would certainly be of great significance for the gas release potential in a repository.

The present study was aimed at a systematic investigation of whether there really is a critical gas pressure of highly compacted bentonite, and to which other properties this pressure is then related. Also, the project should give evidence of whether possibly existing critical gas pressures are the sum of the "true" critical pressure (at no water backpressure) and an applied backpressure. Furthermore, it should be demonstrated whether possibly existing critical gas pressures are intrinsic material parameters or whether they depend on the size of the sample investigated.

2 TEST PROGRAM

The experiments comprised of the individual tests that are specified in Table 1. They were all run at the Swedish Geological company's laboratory in Lund with the exception of the hydrogen gas test, which was conducted at the University of Luleå.

Table 1. Test specification

Test no	Bulk density* ρ_m, t/m^3	Swell. pressure	Back-pressure	Hydr. conduct.	Gas conduct.	Sample height, cm
1	2.08	x	-	x	N_2	1.5
2	2.02	x	-	x	N_2	1.5
3	1.88	x	-	x	N_2	1.5
4	1.92	x	x	x	N_2	1.5
5	1.70	x	x	x	N_2	1.5
6	2.14 (2.20)	x	-	-	N_2	2.0
7	2.10	-	-	-	N_2	30.0
8	2.12	-	-	-	H_2	1.5

* water saturated state

The physical processes associated with gas percolation through highly compacted bentonite have not been evidenced in earlier investigations and steps were therefore taken in the present study to identify the major mechanisms involved in such percolation. For this purpose, specimens were cut from tested samples for microscopy, and this required application of suitable embedding and preparation techniques. Only one sample, percolated with nitrogen gas and with a bulk density of 1.92 t/m^3 was investigated, this study being preceded by a series of tests to check various embedding substances in order to avoid formation of structural artefacts.

3 TEST EQUIPMENTS AND PROCEDURES

3.1 Experimental set-up

3.1.1 Oedometers, sample preparation

The LuH oedometer (Fig 1) was used in all the experiments except for Test no 7, for which a specially designed device was manufactured.

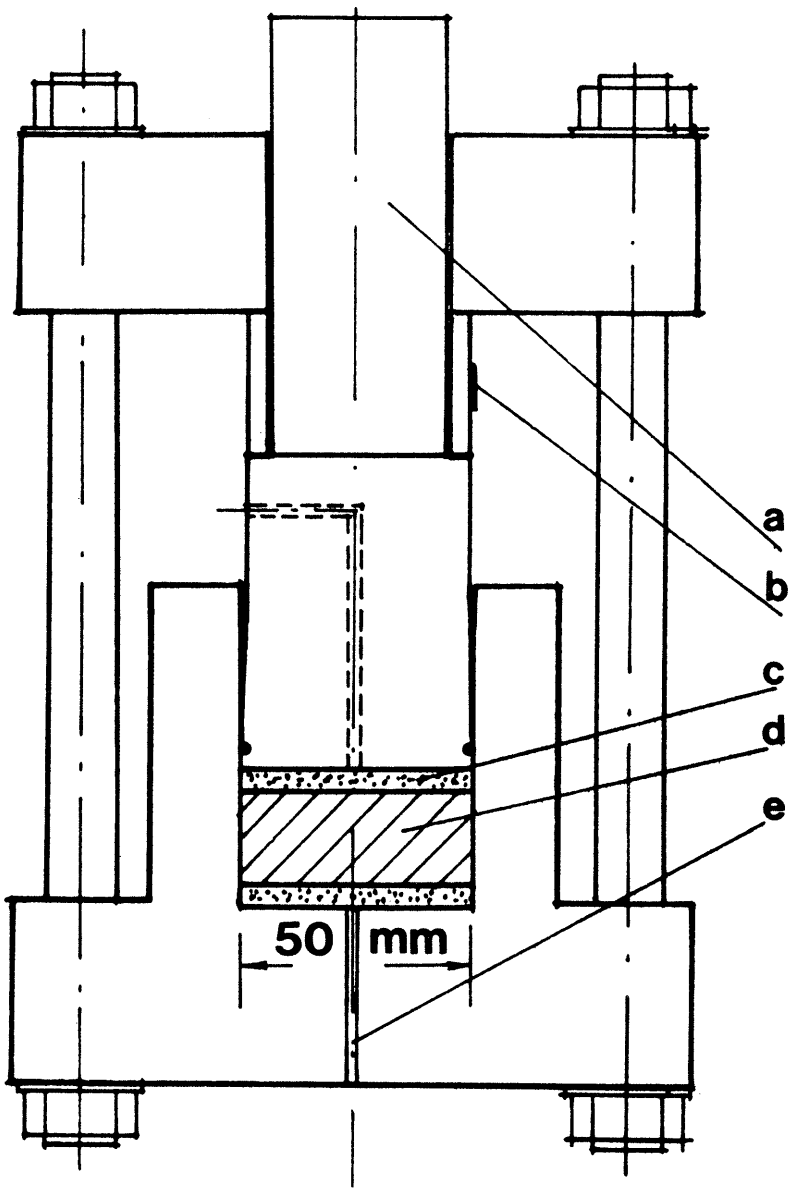

Fig. 1. The LuH oedometer. a) Piston for loading the sample. b) Strain gauge glued to the ring. c) Filter stone. d) Sample. e) Water inlet

The samples investigated in the LuH oedometer were prepared in two different ways, either by applying precompacted, well fitting specimens in the oedometer and locking the piston in a position which

allowed the samples to swell to a preset volume and density by adding water, or by compacting air-dry bentonite powder directly in the oedometer. Both techniques seem to yield the same swelling pressures and conductivities. For saturation, water was let in at the lower end while the upper was left open for air release. In the course of the saturation, the swelling pressure was determined by loading the piston so that the ring became almost stress-free, at which moment the applied, measured force was equal to the swelling force (3). Full saturation was indicated by a constant swelling pressure at successive determinations. After one to two weeks of rest to yield improved structural homogeneity, the hydraulic conductivity and then the gas conductivity were measured. The loading phase is shown in Fig 2.

The 30 cm long clay sample (Test no 7) was confined in the permeameter shown in Fig 3. The photograph illustrates the gas percolation test stage.

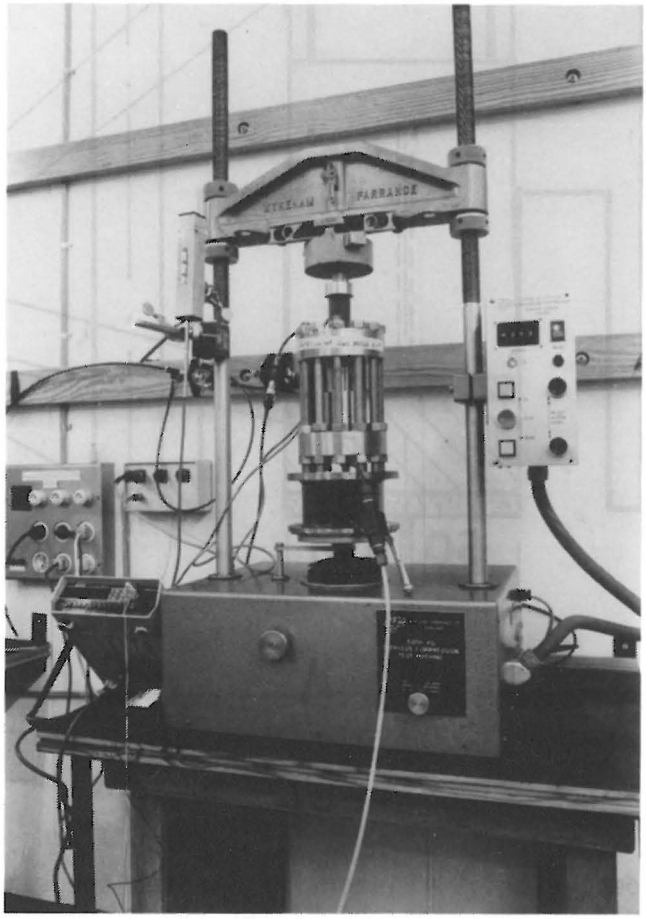

Fig. 2. The loading machine with the load cell on top of the oedometer.

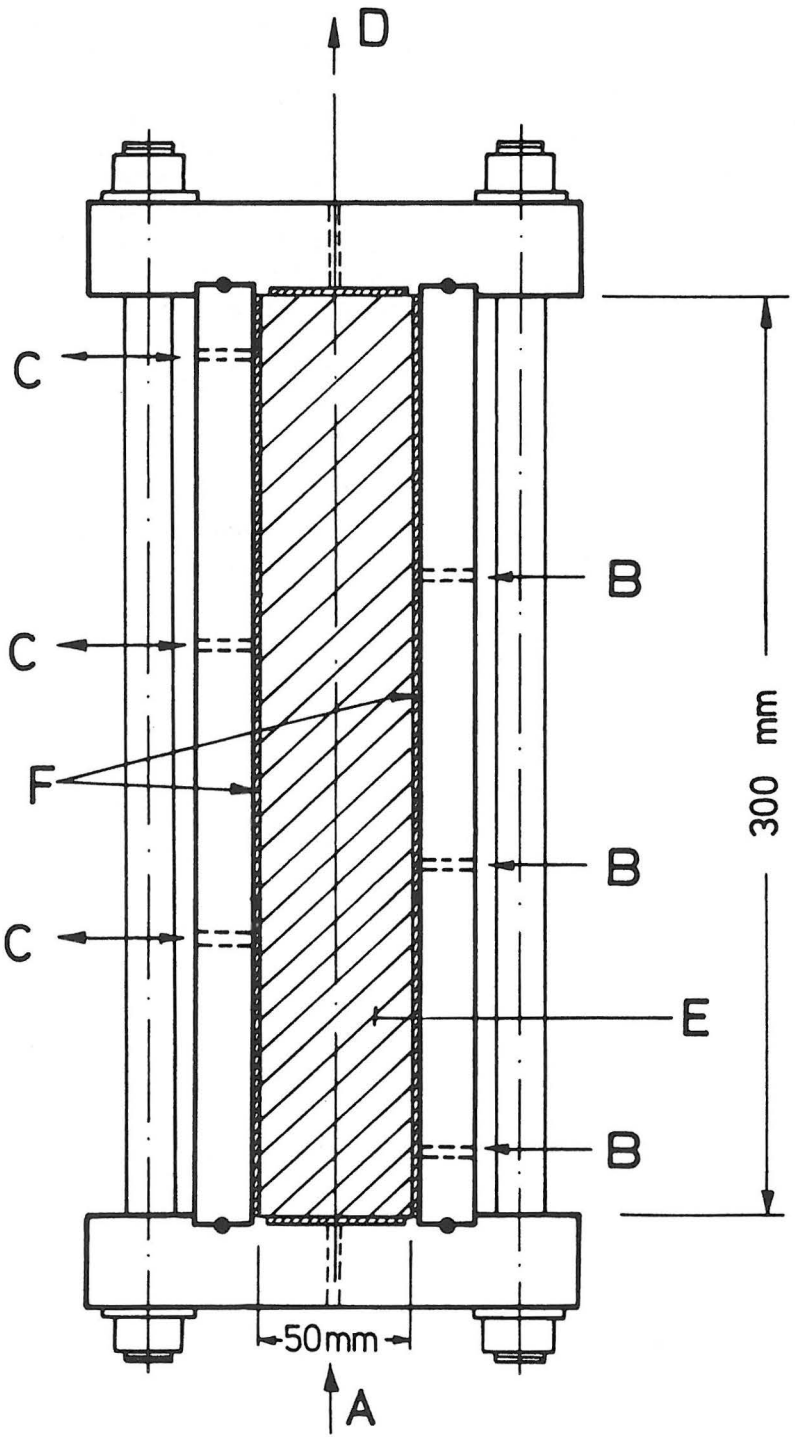

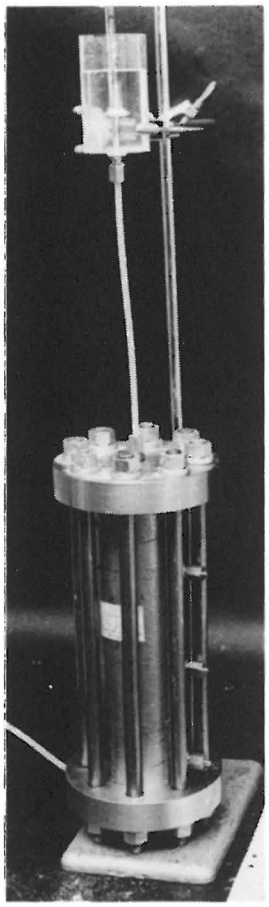

Fig. 3. Design of the long permeameter. A) Gas inlet in conductivity test. B) Water inlets for saturation. C) Air outlets during saturation. D) Gas outlet in conductivity test. E) Bentonite sample. F) Filters.

In order to reach full saturation in a reasonably short time the long clay sample, which consisted of 20 1.5 cm thick precompacted discs with an initial water content of about 11 %, had to be supplied with water at the periphery. This required the use of a circumferential filter which had to be separated from the end filters to prevent gas leakage in the conductivity test phase. Water saturation was assured by checking the daily water uptake from the B inlets, full saturation being indicated by no further water migration. This stage was reached after slightly more than 3 weeks, which is in agreement with theoretical predictions assuming the process to be one of diffusion. After this stage the permeameter was disassembled and the sample extruded. The filter was removed and the sample again emplaced in the metal cylinder, after which the space between sample and confinement was filled with an epoxy resin that expands slightly on hardening. This secured that no gas leakage could take place along inner vertical interfaces between the various components at the subsequent gas pressure test.

3.1.2 Water

The water used for saturation of the clay was delivered by NAGRA and de-aired in the SGAB laboratory before use. It has a relatively high salinity, the composition being given by Table 2.

Table 2. Ionic composition of NAGRA reference water ("Project Gewaehr") according to NAGRA

Cations (mg/l)	
Na	4038
K	45
Mg	2.6
Ca	870
Sr	21
Fe (tot)	0.45
Mn (tot)	3.1
Anions (mg/l)	
Cl	6620
F	3.6
SO_4	1560
Alcalinity	1.58 meq/l
Dissolved carbonates	1.91 mmol/l
Others	
SiO_2	17 mg/l
U	10^{-4} mg/l

3.2 Hydraulic conductivity testing

Although it was not part of the original program, an estimation of the hydraulic conductivity was made prior to the gas conductivity tests. For this purpose the water pressure at the lower inlet of the oedometer was increased to about 20 kPa at maximum, the outflow through the piston being measured by recording the time-dependent displacement of the air/water meniscus in a calibrated capillary tube.

While the hydraulic gradients in earlier water percolation tests had usually been very high (4), they were kept lower in the present experiments in order to make them better related to the actual hydraulic conditions in deep-sited repositories. At higher bulk densities the percolation rates were thereby reduced so much that a light microscope had to be used to measure the rate of displacement of the meniscus (Fig 4). The accuracy of the flow rate measurement and the evaluated hydraulic conductivity, which is given in Table 4, is estimated at about 5×10^{-14} m/s.

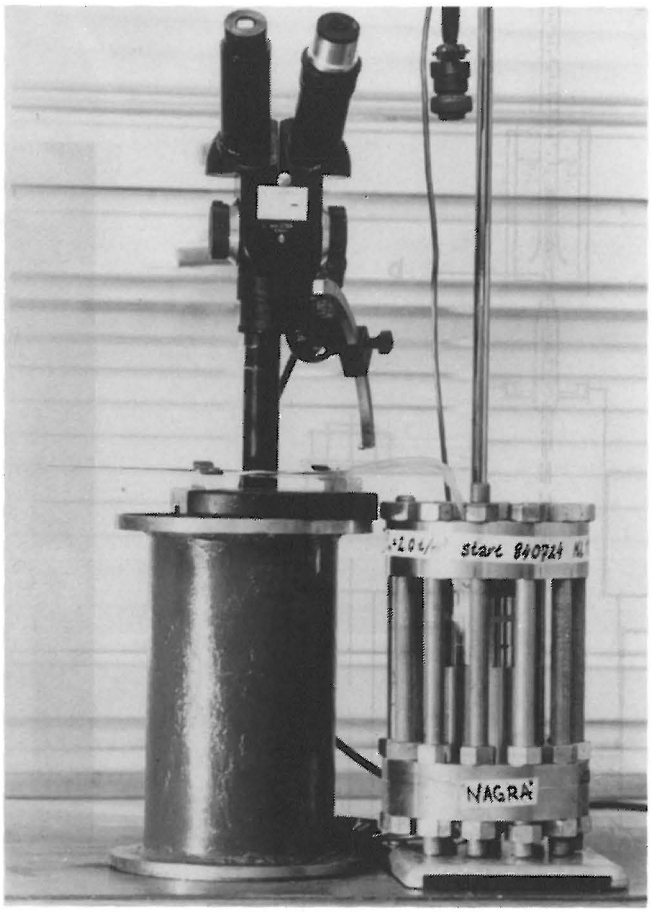

Fig. 4. Arrangement for precision measurement of the hydraulic conductivity. A capillary tube connected with the outflow end of the oedometer and equipped with a micrometer scale is mounted on the microscope table.

3.3 Gas conductivity testing

3.3.1 Recording

The experimental set-up in Tests no 1, 2, 3, 6, 7, and 8 was identical to that used in the earlier study (1), i.e. the gas was let in at the lower end of the permeameters while it was collected in a burette at the upper end (Fig 5) arranged so as to pick up transferred gas and storing it at a pressure that was not very different from atmospheric. Before starting the gas experiments, the lower filter was first drained by evacuation so that gas could be in direct contact with the saturated clay at the upper boundary of the filter.

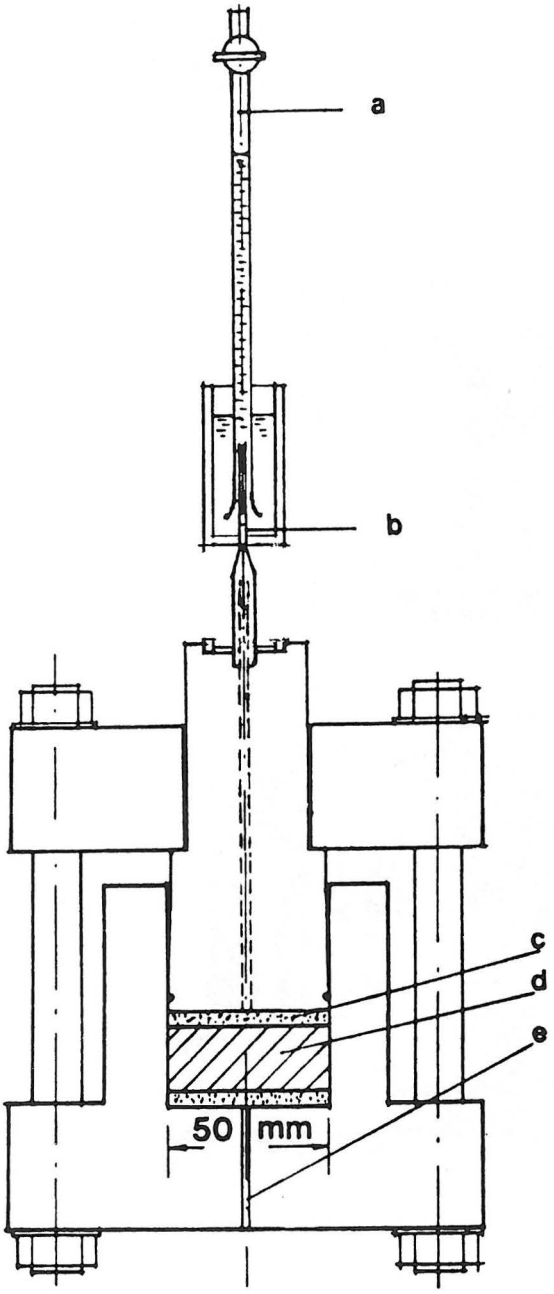

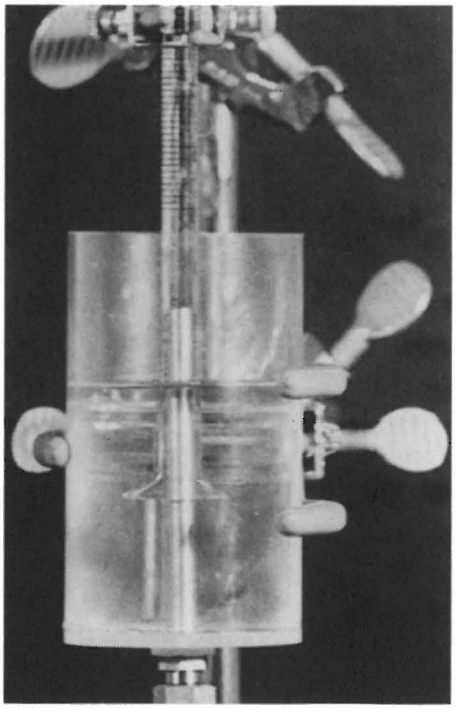

Fig. 5. Gas collecting device. a) Burette for gas collection, b) Syringe, c) Filter, d) Clay sample, e) Gas inlet

In the backpressure tests, a water pressure was applied at the upper end of the samples. It was taken to be sufficiently high - 1 to 3 MPa - to demonstrate whether the recorded net critical pressure is actually the sum of the "true" critical pressure and the water backpressure. This pressure was produced by a Haskel pump fed by a bask with non-pressurized water (Fig 5). The pump was attached to a pressure vessel which was connected to the outlet from the permeameter, and which was also equipped with a burette for gas accumulation. The determination of critical gas pressures did not require accurate determination of the volume of percolated gas; it was simply signalled by a sudden gas break-through manifested by a fast gas bubble travelling into the burette. The procedure at the gas conductivity test was to apply, simultaneously and stepwise, equal water and gas pressures up to a certain value, and then increasing the gas pressure beyond that water pressure.

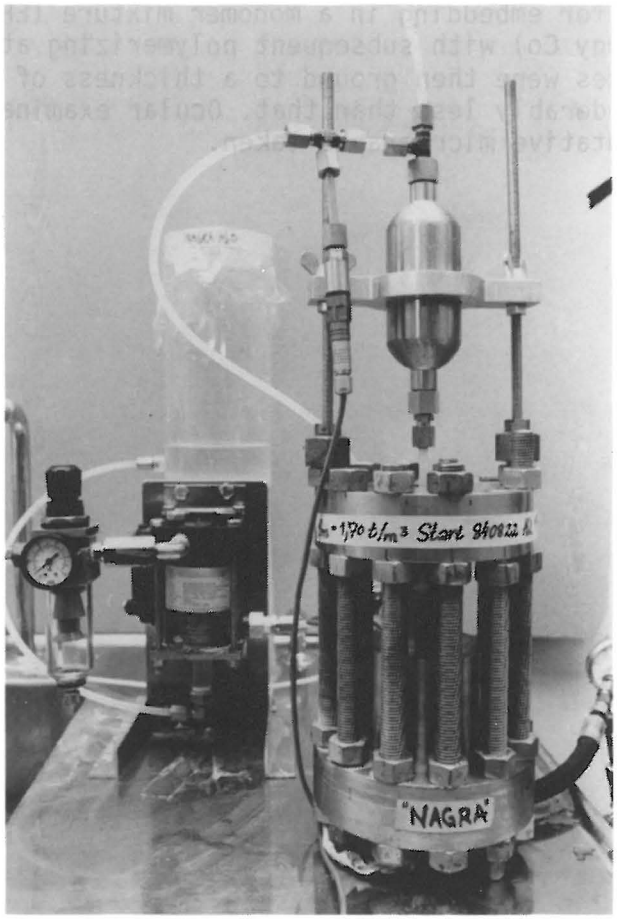

Fig. 6. Experimental set-up at backpressure testing. The "boiler"-like pressure vessel is seen right on top of the oedometer. The Haskel pump with its feeding, non-pressurized water tank is seen to the left.

The gas pressure regulation system for keeping the pressure at the required level with reasonable accuracy consisted of a fine-adjustment valve and a pressure indicator with a Kistler piezo-resistive transducer Type 4043 attached to an amplifier and a digital multimeter (voltage). In the backpressure tests a second transducer of the same type was used for recording the water pressure.

3.3.2 Microstructural investigations

It was expected that a qualitative measure of the physical character of the gas penetration could possibly be gained from microscopic examination of thin sections of specimens extracted from gas-percolated samples. The original plans were to prepare ultra-thin sections (300 Å) for transmission electron microscopy but in the course of the investigation the microstructural changes caused by penetrated gas turned out to be so obvious that ordinary 30 µm sections examined by light microscopy were better suited.

Specimens were carefully trimmed to a thickness of a few hundred microns for embedding in a monomer mixture (EPO-TEK 301,Epoxy Technology Co) with subsequent polymerizing at 50°C. The hardened pieces were then ground to a thickness of 30 µm, wedging out to considerably less than that. Ocular examination was made and representative micrographs taken.

4 TEST RESULTS

4.1 Swelling pressure

In most of the tests the saturation was associated with swelling and the corresponding coupled water uptake was measured and compared with the predicted rate. Full saturation was reached in 5 to 10 days of the ∅ 50 mm, 15 mm high samples, the successive approach to a final, steady swelling pressure being illustrated by Figs 7-9. Twin tests with and without rubber sealings at the interface between the oedometer ring and the clay sample were run with approximately the same results.

The accuracy of the evaluated pressures is determined by the sensitivity of the load cell and by the elasticity and possible excentricity of the piston/ring/sample arrangement. The conclusion from many test series in Sweden is that the recorded values for higher densities represent a slight overestimation of the swelling pressure, probably by 10-20 %. At low densities the accuracy is low and the true value may be underestimated. Only uncorrected values are given in this report; they are collected in Table 3.

Table 3. Evaluated swelling pressures

Test no	Bulk density ρ_m, t/m³	Swelling pressure Ps, MPa	Remark
1	2.08	26	
2	2.02	18	
3	1.88	1.8	
4	1.92	2.7	
5	1.70	0.1-0.2	
6	2.14 (2.20)	35-45	estimated
7	2.10	25-30	estimated
8	2.12	30-40	estimated

It is concluded that the swelling pressure of the samples with densities equal to and exceeding 2.0 t/m³ is almost identical with that of the KBS samples saturated with the only slightly brackish "Allard water" (3). This verifies that pore water chemistry is not a determinant of the swelling pressure at high bulk densities. As to lower densities we see that the p_s-values are considerably lower than those recorded with the KBS reference water and this confirms the expected colloid chemical effect of the salt NAGRA water, i.e. a rather strong aggregation or coagulation.

It should be mentioned that Test no 6 was originally planned to be run with a bulk density of about 2.2 t/m³. It turned out, however, that the swelling pressure was as high as 90 MPa and that gas pressures exceeding 20 MPa were required to achieve gas breakthrough. Since no such high-pressure gas accumulators are commercially available in Sweden the test was conducted using a sample with a slightly reduced bulk density, i.e. 2.14 t/m³. Its swelling pressure was not determined here but the comprehensive research in this field indicates a swelling pressure in the range of 30-45 MPa. The corresponding pressures for tests no 7 and 8 were also estimated.

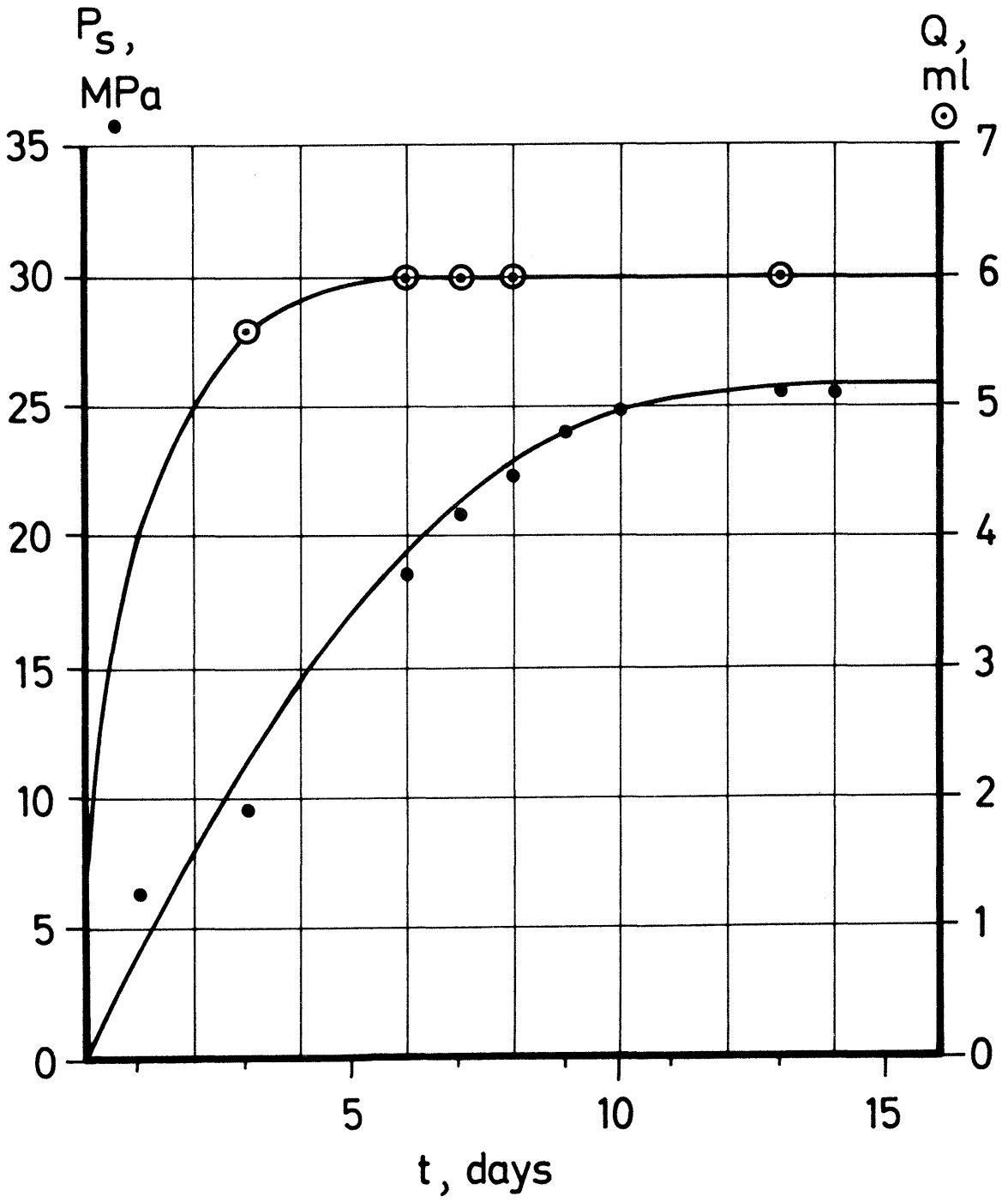

Fig. 7. Development of swelling pressure (·) and water uptake (⊙) in Test no 1 (ρ_m = 2.08 t/m^3)

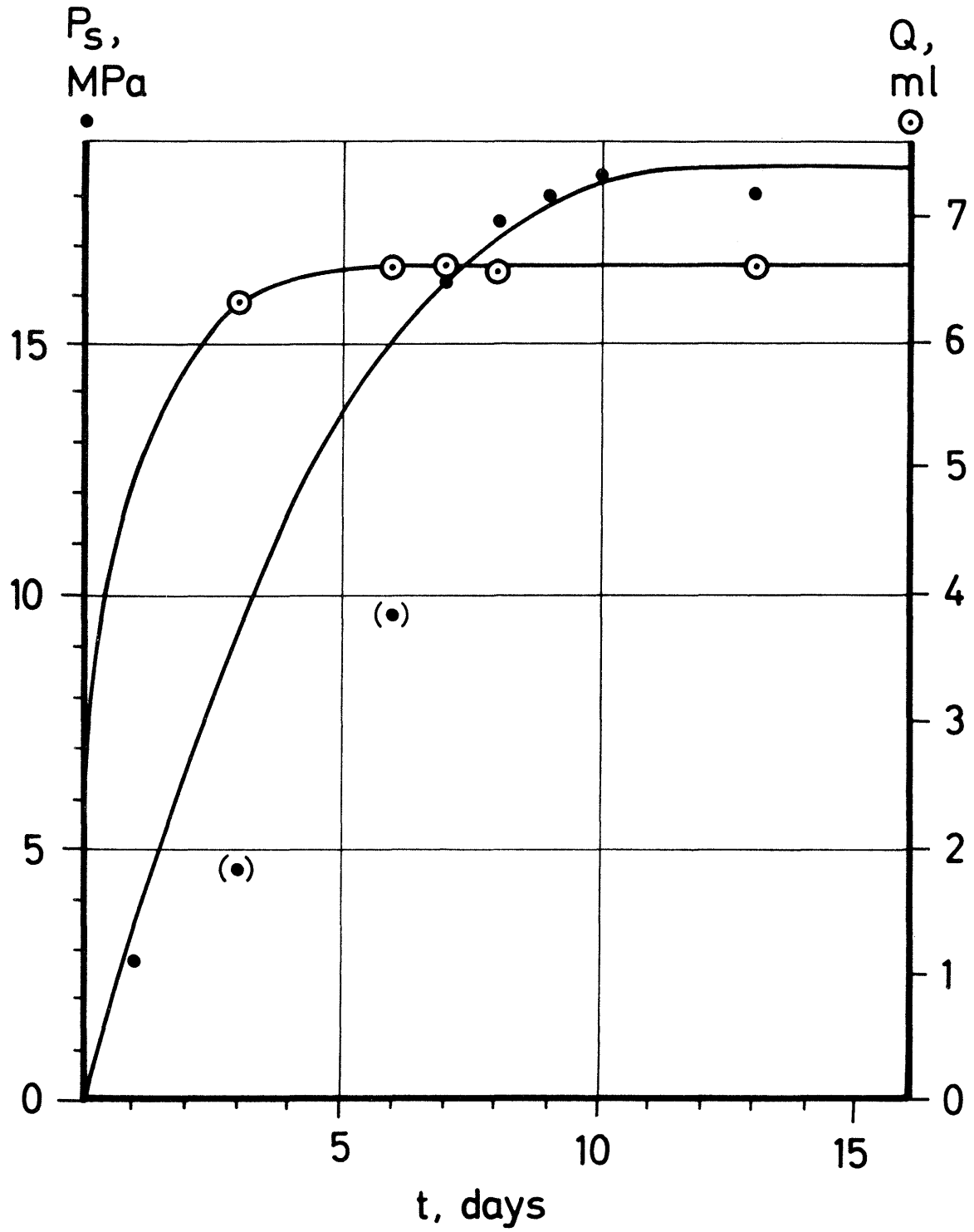

Fig. 8. Development of swelling pressure (·) and water uptake (⊙) in Test no 2 (ρ_m=2.02 t/m³)

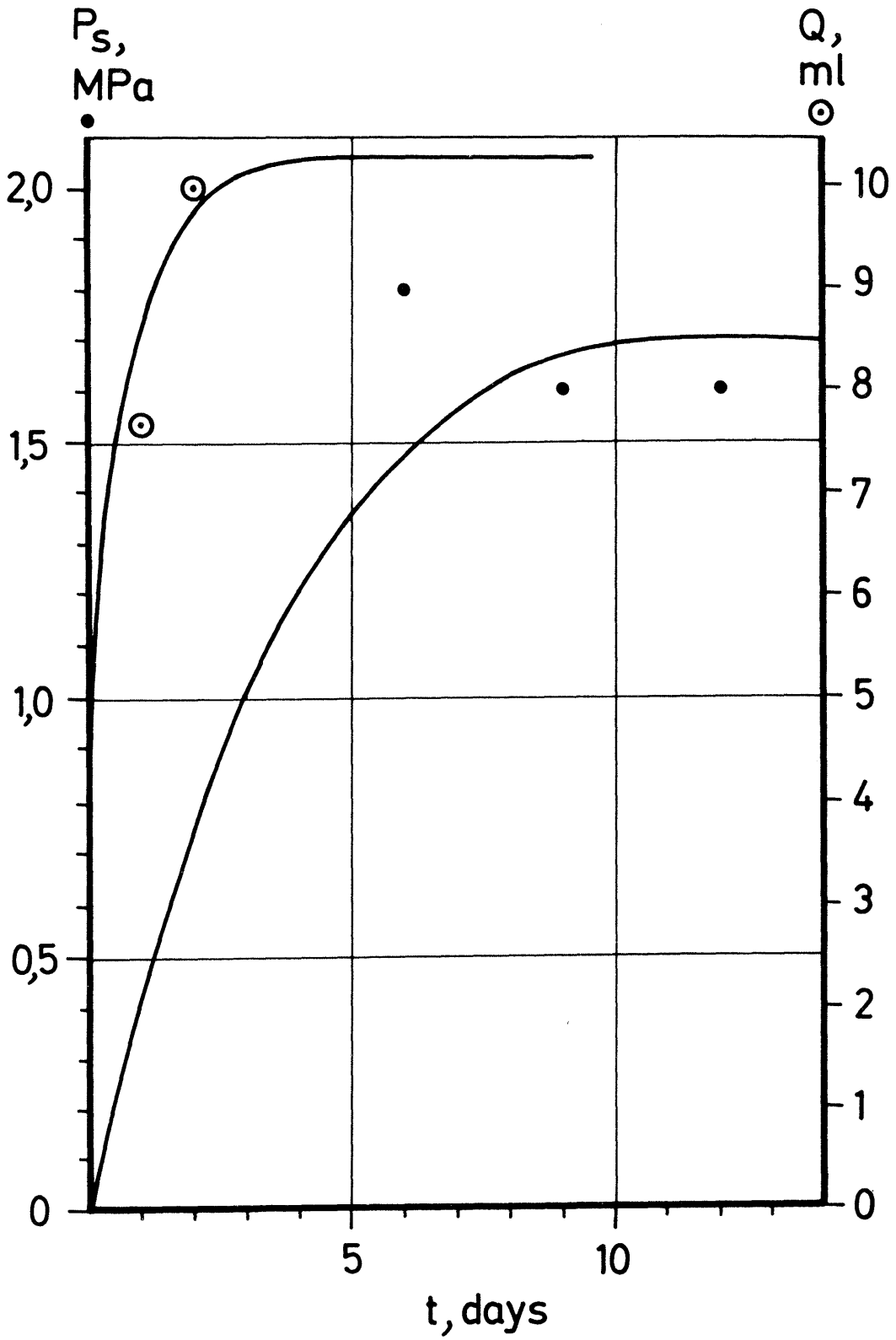

Fig. 9. Development of swelling pressure (·) and water uptake (⊙) in Test no 3 (ρ_m=1.88 t/m³)

4.2 Hydraulic conductivity

The results of the water percolation tests are compiled in Table 4. In tests no 1 - 4 the hydraulic conductivity was concluded to be equal to or less than 10^{-13} m/s and of the same order of magnitude as the estimated accuracy of the experimentally determined values. This suggests that the conductivity in this density range is about the same as that obtained in the KBS "Allard water" study. At lower bulk densities the "NAGRA water" samples are more permeable, however, which is caused by the salt-induced, more aggregated microstructural pattern. It yields larger and many more micropores than when "Allard water" is used for saturation.

Table 4. Hydraulic conductivity k, m/s

Test no 1, ρ_m = 2.08 t/m³

Time after onset or change of hydraulic gradient	Hydraulic gradient	k m/s
24 hours	133	$< 10^{-13}$
48	133	$< 10^{-13}$
168	133	$< 10^{-13}$

Test no 2, ρ_m = 2.02 t/m³

Time after onset or change of hydraulic gradient	Hydraulic gradient	k m/s
2.5 hours	133	$< 10^{-13}$
3.4	133	$< 10^{-13}$
4.4	133	$< 10^{-13}$
23	133	$\sim 10^{-13}$
47	133	$\sim 10^{-13}$

Test no 3, ρ_m = 1.88 t/m³

Time after onset or change of hydraulic gradient	Hydraulic gradient	k m/s
24 hours	133	$\sim 10^{-13}$
48	133	$\sim 10^{-13}$
72	133	$\sim 10^{-13}$
24	65	$< 10^{-13}$
48	65	$< 10^{-13}$
72	65	$< 10^{-13}$

Test no 4, ρ_m = 1.92 t/m³

Time after onset or change of hydraulic gradient	Hydraulic gradient	k m/s
24	133	$< 10^{-13}$
48	133	$< 10^{-13}$
120	133	$< 10^{-13}$

Test no 5, ρ_m = 1.70 t/m³

Time after onset or change of hydraulic gradient	Hydraulic gradient	k m/s
19	133	4×10^{-11}
26	133	4×10^{-11}
43	133	4×10^{-11}
65	133	4×10^{-11}
87	133	3×10^{-11}

4.3 Gas conductivity

4.3.1 General

The gas pressure was increased stepwise and kept constant for 1-5 days at each level in order to find out whether there is a "true" critical pressure and if it is related to any particular soil data. In all the tests such critical pressures were manifested by a suddenly appearing gas bubble release through the outlet tubing. The critical pressure and the gas flow at sub-critical pressures in the eight tests are reported in the subsequent text.

Fig 10 shows a sequence of gas bubbles emanating from the percolated clay.

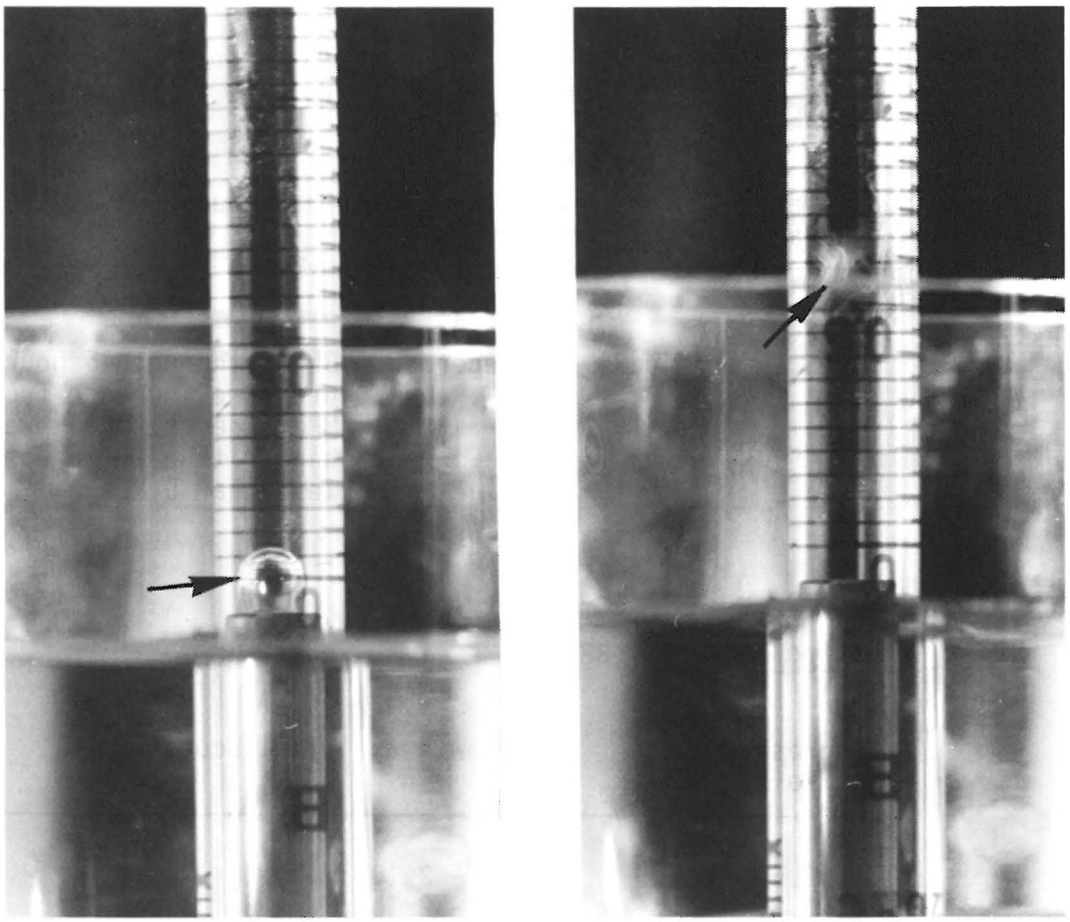

Fig. 10. Rapid bubble release as evidence of gas break-through at the critical pressure. Arrows point at bubbles.

4.3.2 Gas percolation data

Test no 1, ρ_m = 2.08 t/m³

Gas pressure, MPa	Gas flow $m^3/m^2,s$	Time*, hours	Remark
4.0	$2x10^{-9}$ - $6x10^{-9}$		Varying flow
5.0 (critical)	$2x10^{-7}$ - 10^{-6}	120	The gas flow increased successively and ultimately resulted in break-through

Test no 2, ρ_m = 2.02 t/m³

Gas pressure MPa	Gas flow $m^3/m^2,s$	Time, hours
2.0	0	24
5.0 (critical)	Not recorded	Break-through 15 hours after pressure increase from 2 to 5 MPa. The critical pressure was higher than 2 MPa but probably less than 5 MPa

Test no 3, ρ_m = 1.88 t/m³

Gas pressure MPa	Gas flow $m^3/m^2,s$	Time, hours
0.6	$8x10^{-10}$- $2x10^{-9}$	11
0.8	10^{-9} - $2x10^{-9}$	61
1.0	$2x10^{-9}$	24
1.6 (critical)		Break-through 1 hour after pressure increase to 1.6 MPa

*Time from beginning of test, resp. change of applied gas pressure

Test no 4, ρ_m = 1.92 t/m³

Gas pressure MPa	Backpressure MPa	Gas flow $m^3/m^2,s$	Time, hours
1.0	1.0	Not recorded	24
3.0	3.0	"	24
4.8	3.8	"	24
5.4	3.4	"	24
5.8 (critical)	3.4	Breakthrough 6 hours after pressure increase to 5.8 MPa. The "true" critical pressure is 5.8-3.4=2.4 MPa	

Test no 5, ρ_m = 1.70 t/m³

Gas pressure MPa	Backpressure MPa	Gas flow $m^3/m^2,s$	Time, hours
0.01 - 0.05	0	0	408
0.2 - 0.25	0	0	72
0.3 (critical)	0		Break-through 2 hour after pressure increase

One week of rest under zero gas pressure with subsequently repeated test with backpressure yielded:

Gas pressure MPa	Backpressure MPa	Gas flow $m^3/m^2,s$	Time, hours
3.0	3.0	Not recorded	24
3.2 (critical)	2.8		Break-through 20 hours after pressure increase to 3.2 MPa. The "true" critical pressure is 3.2-2.8 = 0.4 MPa

Test no 6, ρ_m = 2.13 t/m³

Gas pressure MPa	Gas flow $m^3/m^2,s$	Time, hours
3-21	0	24
21 (critical)		Break-through immediately after pressure increase to 21 MPa

Test no 7, ρ_m = 2.10 t/m³ (long cylinder)

Gas pressure MPa	Gas flow $m^3/m^2,s$	Time, hours
2	0	72
4	0	96
6	0	48
8	$1.1x10^{-10}$	72
11		Break-through a few hours after pressure increase to 11 MPa

Test no 8, ρ_m = 2.12 t/m³ (Hydrogen gas)

Gas pressure MPa	Gas flow $m^3/m^2,s$	
1	$2x10^{-11}$	
3	$5x10^{-11}$	
5	$8x10^{-11}$	
11	$8x10^{-10}$	
15	$2x10^{-9}$	
19	$4x10^{-8}$	The largely increased gas flow indicates initiation of gas break-through

4.3.3 Microstructural observations

Samples from Test no 3, with ρ_m=1.92 t/m³, were used for microstructural analyses. An immediate observation was that a few gas bubbles emerged from the tiny specimens when they were immersed in the monomer compound. Fig 11 shows a representative micrograph of such a specimen. The picture reveals a few major gas bubbles and a number of almost equally sized, small bubbles, some of which can be seen to emanate from the interior of the clay and which therefore demonstrate that the gas does not consist of air that adheres to the surface of the clay specimen. The micrograph was taken after solidification of the embedding polymer.

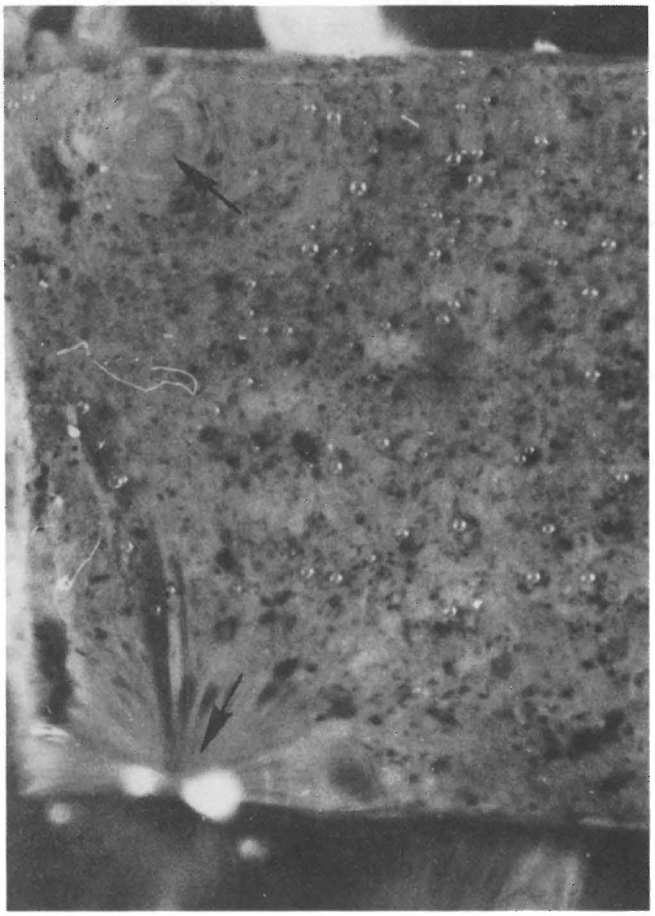

Fig. 11. Micrograph of epoxy-embedded MX-80 specimen, arrows pointing at (non-focused) larger bubbles. The bulk density of the gas-percolated sample is 1.92 t/m^3. (Magnification 30x; all photos in this report taken by Anja Rosenberg, Dep. of Geology, University of Lund).

Examination of thin sections in polarized light verified that the clay had been penetrated by gas which was locked in the sample in the form of small gas-filled voids (Fig 12). The thinner part of the section exhibits numerous minute intersected gas voids while fewer and larger features are seen in the thicker part of the section.

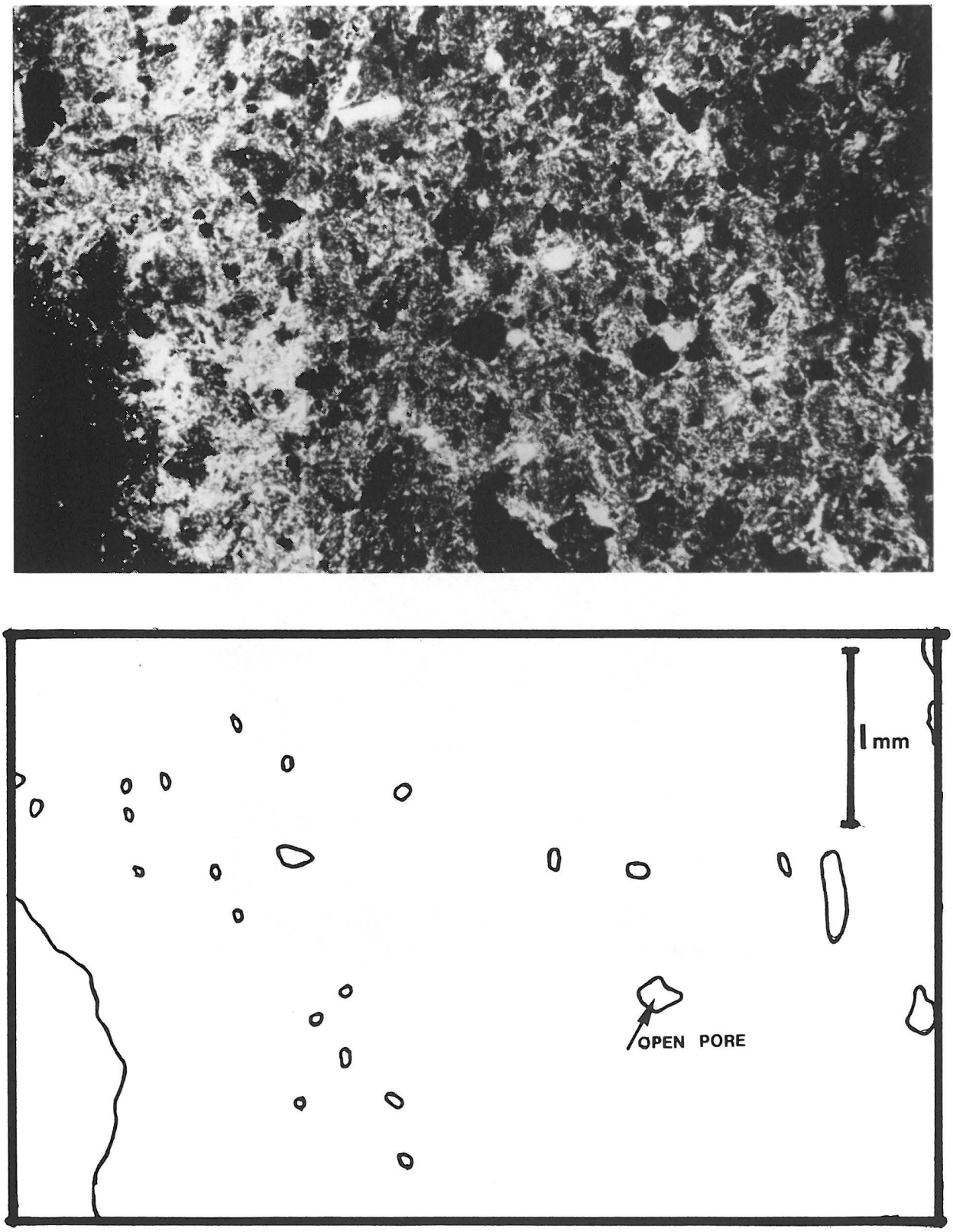

Fig. 12. Thin section of epoxy-embedded MX-80 specimen (30x). Upper picture shows micrograph while the lower one is a graphical interpretation. The left part of the section is wedging out to a rather extreme thinness and shows numerous gas-filled voids, while the right part is 30 µm thick. The large variation in black/white intensity is due to particle orientation effects in polarized light (Crossed nichols).

5 CONCLUSIONS

5.1 Hydraulic conductivity

Experience from earlier, systematic studies of the hydraulic conductivity shows that the electrolyte concentration of the pore water is a determinant of the hydraulic conductivity. In principle, a high concentration at low bulk density yields a porous and permeable particle network (Fig 13), while at high bulk density the microstructural pattern is less but still somewhat influenced by the pore water chemistry as indicated by the KBS study of Na and Ca bentonites (Fig 14). /See (4)/.

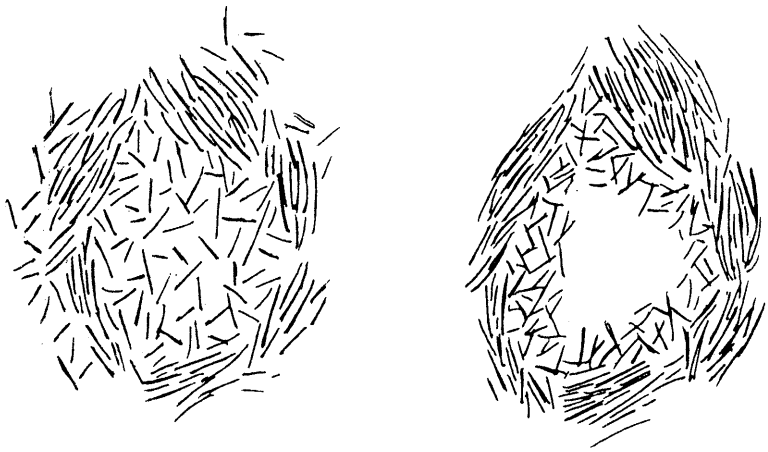

Fig. 13. Influence of pore water salinity on the clay particle arrangement at low bulk density. Left: low salinity; Right: high salinity.

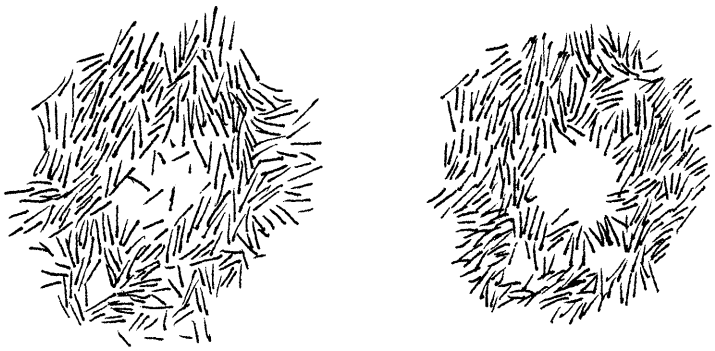

Fig. 14. Influence of pore water salinity on the clay particle arrangement at high bulk density. Left: Low salinity; Right: high salinity.

The structural models imply that the hydraulic conductivity is very much dependent of the type and concentration of dissolved cations at low bulk densities and they logically explain that the presently investigated 1.7 t/m^3 sample saturated with NAGRA water is relatively permeable.

In water saturated smectite-rich clay with a low or moderate bulk density, the water percolation driven by a hydraulic gradient is relatively uniformly distributed over a cross section. However, at higher densities than about 1.8 t/m^3 the massive clay aggregates let very little water through while it still migrates through the more or less continuous inter-aggregate pores which form more or less tortuous passages. This yields a non-uniform percolation which is expected to be particularly pronounced at very high densities. It is important in this context to realize that the microstructure will be heterogeneous and contain micropores with diameters ranging between a few tens and a few thousands of Ångström units even when the density of the saturated clay exceeds 2.2 t/m^3 (5), (6).

5.2 Gas conductivity

The present study shows, beyond doubt, that there is a critical gas pressure. If this pressure is exceeded and kept constant, a successively increased gas flow takes place in the course of which the gas passages become widened. The pressurized gas first tends to pass through the widest available continuous passage and when the water in this particular passage is expelled it serves as an effective gas drainage, which may be sufficient to let all produced gas pass through as long as its pressure is sufficiently high. In practice, there will be a number of almost equally effective passage-ways, as demonstrated by Fig 11, but only a very small fraction of the cross section will actually be penetrated. This verifies that a fairly small part of the pore water will be expelled initially at gas break-through. As to the gas migration at pressures lower than the critical pressure, diffusion of dissolved gas is probably of major importance.

Separate, recent gas migration studies in Sweden indicate that the major resistance to gas penetration at very low clay gel densities (1.3-1.7 t/m^3) is negative pore pressures in capillary-like continuous voids that are common microstructural features in such gels. At high bulk densities the gas, which probably propagates in a finger-like manner, has to displace closely located aggregates to make its way. This suggests that the critical gas pressure should then be related to the swelling pressure. The relationship between the critical gas pressure and the swelling pressure is given in Table 5. It demonstrates that the p_c/p_s-ratio is lower than unity and in the range of 0.2-0.9 except in the case of the lowest density at which the swelling pressure may not have been a determinant of the critical gas state.

The low p_c/p_s-ratio of Test no 1 and 2 may be explained by the rapid pressure increase. Thus, the hydrogen gas experiment and certain other gas tests indicate that a successively increased gas pressure with small increments produces a "pseudo-critical pressure" which is higher than the critical pressure obtained at large pressure steps. This is analoguous to the development of "pseudo-consolidation" pressures at small load increments of an oedometer-compressed sample. It is due to a successive microstructural rearrangement and self-healing caused by displacement of small

aggregates which can be moved by the penetrating gas to clog narrow passages. For a real repository with slow gas pressure build-up it is therefore reasonable to assume that the critical gas pressure is slightly higher than the laboratory-derived ones.

Table 5. Ratio of critical gas pressure (p_c) and swelling pressure (p_s)

Test no	Bulk density t/m^3	p_c/p_s
1	2.08	0.2
2	2.02	0.3
3	1.88	0.9
4	1.92	0.9
5	1.70	2-4
6	2.14	0.5-0.6
7	2.10	0.4-0.5
8	2.12	0.5-0.7

The gel-displacing effect of penetrating gas has been documented through a number of microscope observations as demonstrated in Fig 15. The micrograph illustrates the formation of a dense, homogeneous zone of aligned particles at the periphery of a gas channel. The zone, which appears grey in the picture (arrows), has optical properties in polarized light which give evidence of dense, shear-induced, face-to-face particle grouping ("domain" formation).

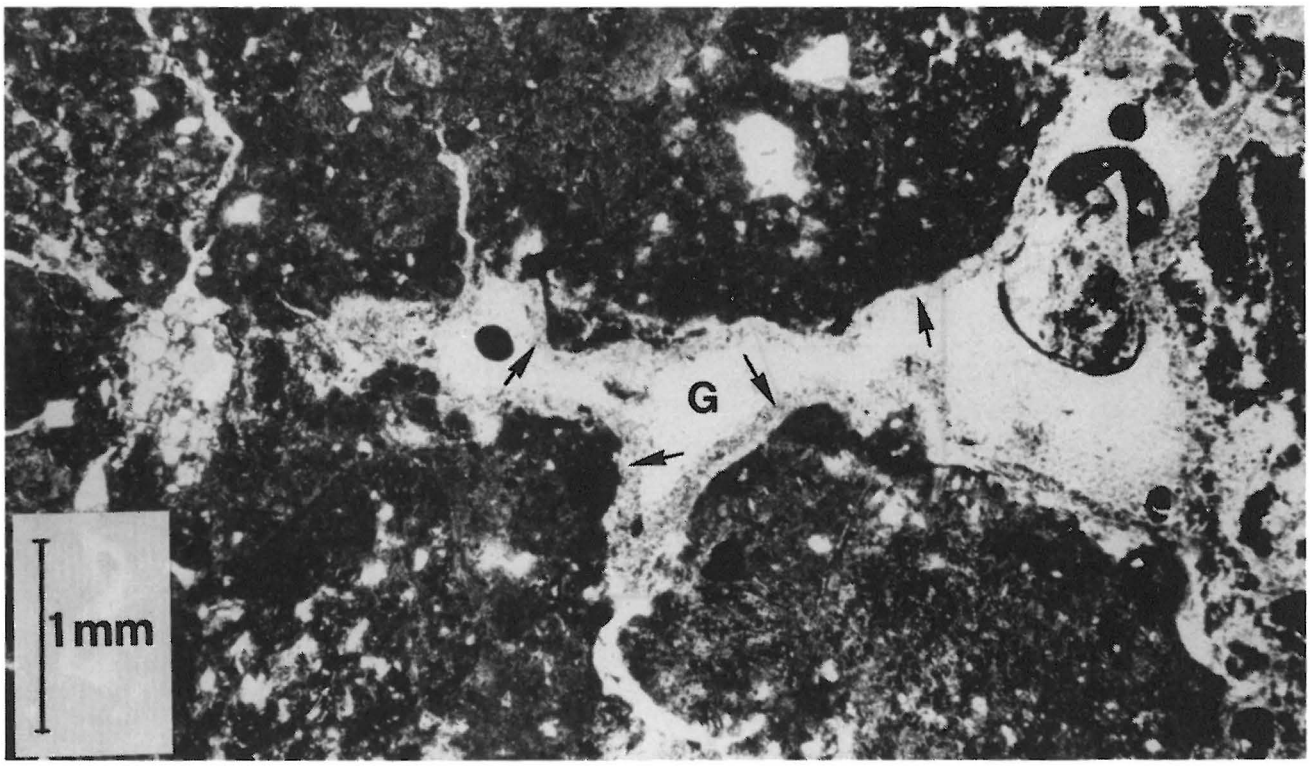

Fig 15. Micrograph of thin cross section (30 μm) of large gas passage through low-density bentonite (ρ_m=1.63 t/m^3). G represents gas channel while the arrows point at clay domains. (Polarized light)

5.3 Stress conditions

Water and gas conduction through highly compacted bentonite depend on and affect the stress situation in the clay/water system. At bulk densities exceeding 2 t/m^3, which is of primary interest in this context, the theoretical average interlamellar space is equal to or less than about 6 Å if all the water is assumed to be uniformly distributed over the entire specific surface area. Since there are inter-aggregate voids of various size which hold "free" water most of the dense aggregates consist of tightly arranged, mutually supporting stacks of parallel smectite flakes with a smaller spacing than 6 Å. This corresponds to one or two layers of water molecules which are strongly held at the minerals. Such dense smectite/water sandwiched systems form a continuous framework with elastic properties much like strong springs and they transfer the so-called effective stress (or "grain pressure" in soil-mechanical terminology) throughout a clay element.

In practice, the strength and rigidity of the individual framework components vary so that stochastic principles have to be used to visualize the stress situation in a clay sample exposed to gas and water backpressures. Thus, due to compositional and density differences and orientation effects, the effective stress over a cross section through a clay sample which exhibits a certain laboratory-derived average swelling pressure actually varies from element to element as illustrated by Fig 16. A considerable part of the right wing of the spectrum represents a mono-layer of interlamellar water, which cannot be expelled at pressures lower than about 200 MPa (7).

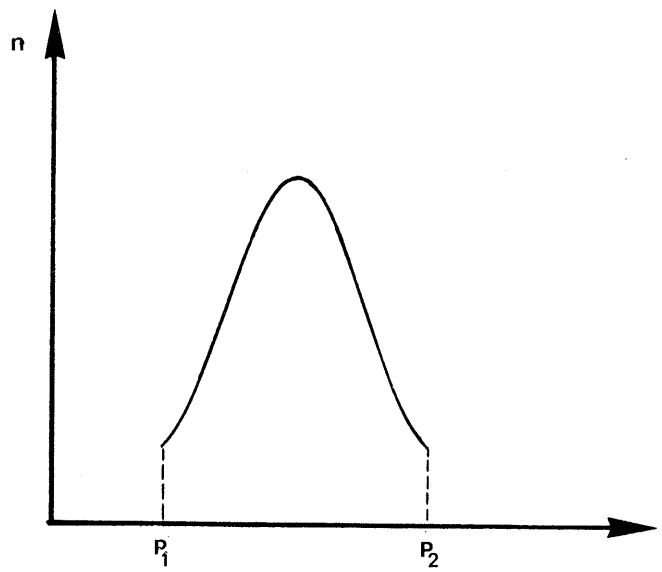

Fig. 16. Hypothetical distribution of the effective stress in the structural components of a clay sample (P_1 and P_2 represent lower and upper percentiles).

Let us now consider the arrangement in Fig 17 which shows a schematic clay structure. As in our tests the gas pressure is initially equal to the backpressure and practically no gas has yet entered the clay. Thus, the water pressure is constant and equal to the gas pressure in all the elements. Since microstructural variations yield a varying effective stress, the probable range being something like 1-50 MPa, the p_s-distribution is of the type shown in Fig 17.

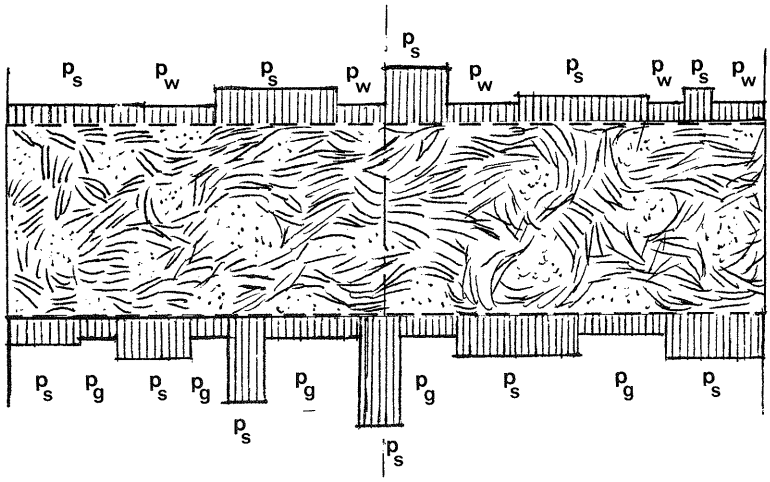

Fig. 17. Stress situation at low gas pressure (p_g) with equal water backpressure (p_w). Dotted areas represent "free" water

The gas pressure is now increased while the water pressure is kept constant and gas displaces water in a number of small voids, the deepest penetration taking place in the widest "channel", i.e. where the resistance to displacement is at minimum (Fig 18). At this stage the gas pressure is constant in the entire channel and in all the voids and the pressure distributions over the boundaries are then those shown in Fig 18.

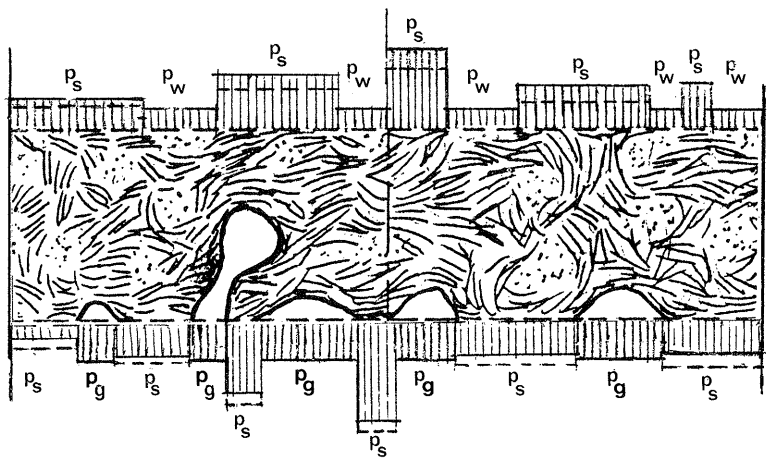

Fig. 18. Pressure distribution at the clay/water and clay/gas interfaces at gas pressure approaching the critical value. The net pressure at the gas/water interface is (p_g-p_w) which is balanced by capillary forces and interparticle bonds

As seen from Figs 17 and 18 the effective stresses, or local swelling pressures, are altered at the upper and lower boundaries of the clay element when the gas pressure is elevated and gas begins to penetrate the clay. This process is associated with capillary effects, which are known to produce compression in soft clays. Because of the strength of large parts of the particle framework of highly compacted bentonite clay, these parts will not undergo compression even at extreme pressures, which means that the clay particle network will continue to fill up practically all of the space and exert a pressure on the boundaries. As indicated by Fig 18, this pressure will be slightly lower on the gas pressure side and slightly higher on the water pressure side. Local compression of less dense particle regions may take place due to this, but the tests discussed in this report demonstrate that such effects do not invalidate the "critical" gas pressure concept. This means that the critical gas pressure represents an intrinsic material parameter in the form of a treshold value, the exceeding of which leads to rapid gas conduction.

6 REFERENCES

/1/ Pusch, R. & Forsberg, Th. (1983): Gas Migration through Bentonite. SKBF/KBS Technical Report 83-71.

/2/ Pusch, R. (1983): Use of Clays as Buffers in Radioactive Repositories. SKBF/KBS Technical Report 83-46.

/3/ Pusch, R. (1980): Swelling Pressure of Highly Compacted Bentonite. SKBF/KBS Technical Report 80-13.

/4/ Pusch, R. (1980): Permeability of Highly Compacted Bentonite. SKBF/KBS Technical Report 80-16.

/5/ Pusch, R. (1967): A Technique for Investigation of Clay Microstructure. Journal de Microscopie, Vol. 6.

/6/ Smart, R. & Tovey, N.K. (1981): Electron Microscopy of Soils and Sediments. Clarendon Press, Oxford.

/7/ van Olphen, H. (1965): An Introduction to Clay Colloid Chemistry. Interscience Publishers.